

BAHOP: Similarity-based Basin Hopping for A fast hyper-parameter search in WSI classification

Jun Wang
City University of HONG KONG
jwang699-c@my.cityu.edu.hk

Yu Mao
MBZUAI
yu.mao@mbzuai.ac.ae

Yufei Cui
McGill University
yufei.cui@mail.mcgill.ca

Nan Guan
City University of HONG KONG
nanguan@cityu.edu.hk

Chun Jason Xue
MBZUAI
jason.xue@mbzuai.ac.ae

Abstract

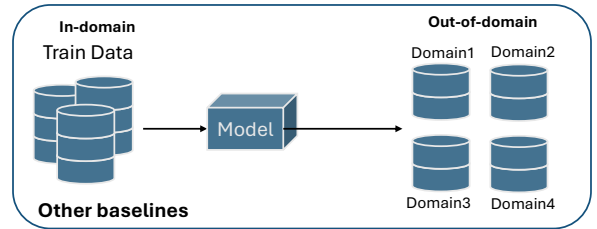
Pre-processing whole slide images (WSIs) can impact classification performance. Our study shows that using fixed hyper-parameters for pre-processing out-of-domain WSIs can significantly degrade performance. Therefore, it is critical to search domain-specific hyper-parameters during inference. However, searching for an optimal parameter set is time-consuming. To overcome this, we propose BAHOP, a novel Similarity-based Basin Hopping optimization for fast parameter tuning to enhance inference performance on out-of-domain data. The proposed BAHOP achieves 5% to 30% improvement in accuracy with $\times 5$ times faster on average.

1. Introduction

Following the success of early computational pathology applications, dataset sizes have increased, prompting more multicentric efforts to address variability in staining, image quality, scanning characteristics, and tissue preparation in different laboratories. This has highlighted a known issue where computational pathology algorithms perform best on data on which they were trained but less well on data from other sources. Generalization continues to pose a major challenge in this field, as significant differences in clinical variables between tissue source sites can adversely affect the performance of histopathological tasks [6, 11, 26].

State-of-the-art multiple instance learning (MIL) models have shown promising improvements in whole slide image (WSI) classification on out-of-domain (OOD) data by training on large, diverse datasets [2, 15, 17, 21, 23, 31]. Out-of-domain classification occurs when a model is trained on one dataset and tested on another from a different domain. For instance, a model might be trained using Camelyon16

Original: Fixed pre-processing hyper-parameter



Optimal: Different hyper-parameter for different domain

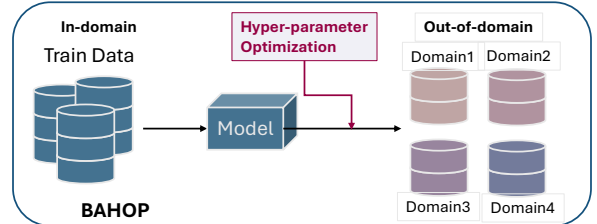


Figure 1. The performance of out-of-domain inference varies with preprocessing parameters across various MIL models and datasets. Consequently, we suggest that each specific center within the dataset should adopt its own preprocessing parameters to maximize performance. The original method involves all centers using fixed default preprocessing hyperparameters, whereas the optimal method allows each center to use its own specific preprocessing hyperparameters determined by our proposed BAHOP.

data [16] and then evaluated using data from various Camelyon17 centers. As indicated in Table 1, the performance of a model trained in Camelyon16 can vary significantly at specific centers within Camelyon17.

We discovered that one factor that leads to unsatisfactory performance is the same inference hyper-parameter across different centers. We evaluate the fixed pre-processing parameters' performance on several sub-datasets. The experiment result shows that fixed pre-processing parameters typ-

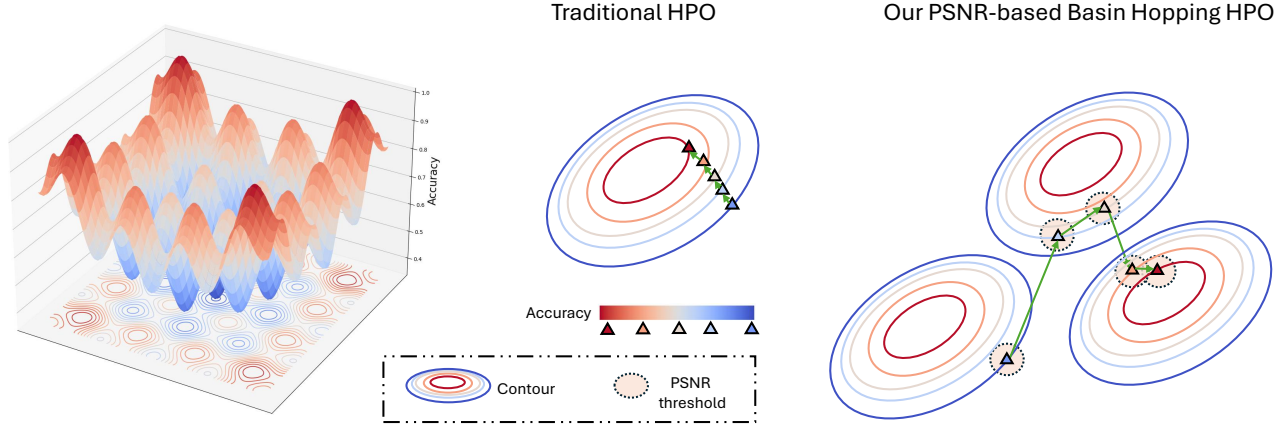


Figure 2. PSNR-based Basin Hopping hyper-parameter optimization for out-of-domain inference in WSIs. The hyper-parameter optimization for the pre-processing task is a non-convex optimization that contains many large local optima. Our BAHOP is developed for fast search, and the jumping range of each iteration is controlled by the PSNR threshold.

ically result in poor out-of-domain performance [11]. For example, MIL models [5, 15, 17] have extremely low accuracy at specific centers within the TCGA [29] and Camelyon17 [16] datasets using fixed parameters. Conversely, tailoring optimal pre-processing parameters for each center significantly improves out-of-domain performance (as illustrated in Figure 1).

Determining optimal pre-processing parameters for histopathological tasks is challenging. The parameter search space is over 10^5 due to the huge size of gigapixel Whole Slide Images (WSIs) and the significant computational resources needed. Previous studies [3] only explore hyper-parameter optimization in learning rates and loss weight coefficients without tailoring their approaches to histopathology applications. When adopting hyper-parameter tuning methods, traditional grid search methods for datasets like Camelyon or TCGA are inefficient, taking several hours to evaluate one parameter group. The whole hyper-parameter space contains hundreds of thousands of possible combinations. Therefore, quicker hyper-parameter search techniques are essential for histopathological tasks.

This paper focuses on how pre-processing parameters influence inference performance, particularly with out-of-domain data, and proposes an efficient parameter search method specifically designed for WSI classification. We propose a Similarity-based Basin Hopping (BAHOP) for Hyper-parameter tuning and improving the accuracy of inferring out-of-domain data across various MIL models and datasets (as shown in Fig. 1). The key contributions of this paper are:

- We have observed that varying pre-processing parameters significantly impact feature extraction and, consequently, model performance—particularly in out-of-domain infer-

ence;

- We present BAHOP, Similarity-based Basin Hopping for fast and effective parameter tuning. This algorithm enhances inference performance at Camelyon 17’s center 1, boosting accuracy from 0.512 to 0.846;
- We expand the proposed BAHOP to include other MIL models using various public datasets, achieving improvements in accuracy ranging from 5% to 30% for out-of-domain data across multiple MIL models and datasets;
- The proposed BAHOP is the first fast hyper-parameter search designed explicitly for histopathological tasks.

2. Related Work

Pre-processing of WSI in histopathology. Variations in tissue processing techniques, including chemical fixation or freezing, dehydration, embedding, and staining, can alter the visual characteristics of the tissue slide in ways that are both non-uniform and non-linear. These changes occur across different tissue types and laboratories [1, 30], consequently, impacting the performance of deep learning. Gurcan et al. [9], Salvi et al. [20], Wang et al. [28] summarize the pre-processing impact for WSI analysis on deep learning frameworks. Tellez et al. quantifies the effects of data augmentation and stain color normalization [14].

There are several research works that specifically explore the issue of dataset bias in computational pathology. Pocevičiūtė et al. [18] quantifies the impact of domain shift in attention-based MIL and points out that MIL performance is worse than what is reported using in-domain test data. Several works [6, 11] discuss bias in histopathological data. Important clinical variables have been shown to be significantly different between tissue source sites, affecting the generalization issue for histopathological tasks.

Table 1. **Performance of Out-of-Domain Inference in Specific Challenging Case.** The performance is reported as the average of Accuracy, AUC, Precision, Recall, and F-score metrics, computed over the 10-fold models.

Model	In-Domain (C16)		Out-of-Domain (C17 Center 1)									
	Acc	AUC	Accuracy		AUC		Precision		Recall		F-score	
			Min	Max	Min	Max	Min	Max	Min	Max	Min	Max
ABMIL	0.901	0.941	0.84	0.92	0.833	0.896	0.788	0.966	0.743	0.829	0.765	0.875
DSMIL	0.925	0.954	0.64	0.89	0.721	0.93	0.491	1.000	0.429	0.943	0.556	0.831
CLAM	0.901	0.946	0.512	0.847	0.708	0.833	0.486	0.839	0.743	1.000	0.648	0.788
TransMIL	0.892	0.935	0.73	0.84	0.861	0.914	0.730	0.823	0.753	0.844	0.724	0.830
Bayes-MIL	0.883	0.916	0.35	0.80	0.819	0.881	0.350	0.759	0.629	1.000	0.519	0.737
MHIM-DSMIL	0.925	0.965	0.77	0.87	0.850	0.921	0.607	1.000	0.600	0.971	0.710	0.800

Hyper-parameters search and optimization in machine learning. [8] propose a Bayes-optimization with Hyper-band strategy and evaluate it in small datasets. [3] search hyper-parameters in per-layer learning rates and loss weight coefficients. These previous works are not designed for histopathology.

Hyper-parameter optimization in histopathological tasks is different than optimization problems in a linear function. The optimization in linear function or small machine learning model with a small dataset can be optimized in many iterations in a short time. However, the optimization in the machine learning model for histopathological tasks is totally different. WSIs are giga-pixel images that demand significantly higher computational resources. Despite advancements in hardware, memory constraints still pose a significant challenge in the digital processing of WSIs in current research [4, 7]. Additionally, nature images have very different data distribution compared to the whole slide image [19]. Therefore, designing a hyper-parameter optimization strategy for computational pathology is necessary. The proposed BAHOP algorithm is the first hyper-parameter optimization strategy designed for histopathological tasks.

3. Motivation and Observation

Public datasets often combine data from various domains [18, 25], obscuring true performance metrics within specific areas. Studies [6, 10, 11] show that domain-specific variations in digital histology can affect the accuracy and bias of deep learning models. In practice, these variations necessitate frequent retraining of models due to changing data domains, which is impractical due to high computational costs. Thus, improving model performance without additional training is essential.

3.1. Pre-processing Impacts Inference Performance for Different Domains.

We found there exists significant variability in inference performance on out-of-domain data across various methods

(refer to Table 1). We employ a grid search to fully understand how pre-processing parameters influence outcomes in center 1 of Camelyon 17 in this motivation experiment. For instance, the CLAM [17] model trained on the Camelyon16 dataset achieves an overall inference accuracy of 0.86 on the entire Camelyon17 dataset but drops to 0.512 at Center 1 of Camelyon17, indicating inconsistent performance. We also evaluate our approach in other centers across different datasets, as detailed in Fig 3 and Appendix. Similar variations are observed across other datasets and MIL models, and the out-of-domain inference is extremely poor in some cases. What’s more, the default pre-processing setting yields varying results depending on the center as shown in Fig 3, where identical hyper-parameters may perform well in one center but poorly in another.

Observation 1 The effect of the pre-processing parameters varies across different datasets. As shown in Fig. 4 and the Appendix, the detection of foreground contours, controlled by several hyperparameters, often results in the exclusion of large areas, which are treated as holes. For instance, adipocyte cells are frequently excluded. However, some tumor cells surrounded by fibers, adipocyte cells, or

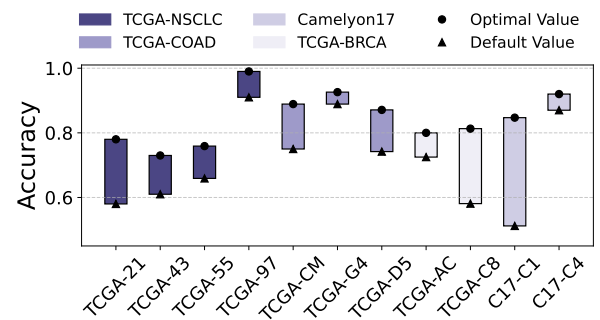


Figure 3. The inference performance of out-of-domain data varies with preprocessing parameters across various MIL models and datasets.

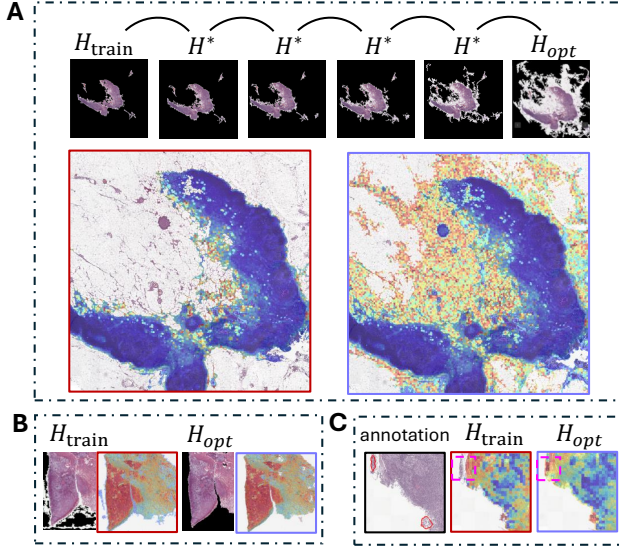


Figure 4. All the heatmaps circled by red boxes correspond to the default hyper-parameter and predict wrong, while heatmaps circled by blue boxes correspond to optimal hyperparameters with correct predictions. Fig.A: Hyper-parameter optimization starts from the default parameter, which is the same as the pre-trained model. The default pre-processed WSI drops many patches that get a high attention score in optimal pre-processed WSI. Fig.B, the dataset is TCGA-NSCLC where dropping tissue can improve accuracy. Fig.C: Some hyper-parameters drop the region of interest(ROI) during pre-processing.

lipid droplets may also be filtered out due to preprocessing parameters and discarded. In Fig. 4(a) and (c), excessive patch removal leads to incorrect predictions, while in Fig. 4(b), it improves prediction accuracy when applied to a different dataset. This variability makes it difficult to quantify the impact of specific patches, especially since the number of patches for a single WSI in a MIL model can exceed 10^5 . While some studies, such as Javed et al. [13], address this issue, there is no consensus on how specific patches influence machine learning models in computational pathology. An adaptive algorithm is needed to address this challenge in histopathological tasks.

Observation 2 Pre-processing optimization is inherently a non-convex problem with numerous large local optima (as shown in Fig. 2). Our objective is to achieve an optimal result with reduced time and computational costs, where this optimum does not need to be a global one.

Rather than identifying specific cell types within tissue areas, we approach this histopathological task from a machine learning perspective. The pre-processing of WSIs focuses on segmenting tissue regions and discarding patches identified as holes or backgrounds. These patches are selected and filtered based on pre-defined parameters, while

most tissue areas containing cells are retained. Consequently, the variations in inference performance caused by multiple interacting hyperparameters can be framed as a hyperparameter optimization problem. This problem can be effectively addressed using an adaptive algorithm tailored for this histopathological task.

3.2. Inefficient Manual Pre-Processing Parameter Search.

In real-world scenarios, retraining machine learning models for every new dataset is often impractical. While optimizing parameter performance is advantageous, finding the optimal settings is highly time-consuming. For instance, evaluating a single set of parameters, including feature extraction, takes approximately 7 hours on an RTX3080 (details in Appendix). Traditional optimization techniques, such as tuning learning rates, batch sizes, or loss weight coefficients, cannot be directly applied to histopathological tasks. Consequently, more efficient parameter search methods are required. Common strategies like grid search demand excessive computational resources and time, rendering them unsuitable for histopathological applications.

Based on these observations, we want to explore three questions.

- Can we improve inference performance on out-of-domain data just by modifying the preprocessing parameters?
- How can we search for parameters more cost-effectively to enhance inference performance?
- Do these observations apply to other multiple instance learning (MIL) models?

Therefore, we introduce our approach in a fast hyper-parameter search in pre-processing parameters of histopathology.

4. Fast Hyper-Parameter Search for Inference Performance in Out-Of-Domain Data

In this section, we formalize hyperparameter optimization and present our BAHOP algorithm step by step. The proposed BAHOP algorithm includes PSNR-based mechanism for limiting the current searching space in each iteration and Basin Hopping to avoid local optima.

4.1. Definition of Problem

A good choice of hyperparameters can significantly improve out-of-domain inference performance, yet optimal hyperparameters vary, depending on the datasets and the models. We assume access to two types of datasets: (1) a large dataset D_{train} for training to produce the foundation model subsequently used to test out-of-domain performance. (2) Multiple subdataset $\{D_{val} = D_{val}^1, D_{val}^2, \dots, D_{val}^n\}$. The validation sub-dataset D_{val} is much smaller than D_{train} and is used only for optimization

at the outer level, not for fine-tuning. Note that these test distributions are distinct and are never shown to the model before the final evaluation.

Let M denote a pre-trained foundation model trained in a large dataset D_{train} with the pre-processing parameter H_{train} . Now, there are many out-of-domain datasets $\{D_{val} = D_{val}^1, D_{val}^2, \dots, D_{val}^n\}$. They are pre-processed by hyper-parameter H_1, H_2, \dots, H_n to obtain the features $F_{val}^1, F_{val}^2, \dots, F_{val}^n$ for inferring. The out-of-domain performance of model M would be tested by the features F_{val}^n that are preprocessed by the hyper-parameter H_n as $y = Infer(H_n, D_{val}^n)$, where y is the performance metric.

We define the histopathological task of identifying the optimal pre-processing for enhanced out-of-domain performance as a hyper-parameter optimization problem, as described in Equation 1, where Φ is the hyper-parameter space. This process helps us determine the most effective final hyper-parameters H_n^* for each validation center D_{val}^n .

$$H_n^* = \arg \max_{H \in \Phi} Infer(BAHOP(H, D_{val}^n), D_{val}^n) \quad (1)$$

4.2. Pre-Processing Problem Modeling

Next, we consider the optimization problem for histopathological tasks. The optimization of H_n is actually the optimization of a combination of pre-processing parameters, not a single variable. Previous pre-processing of WSIs encompasses a series of standard procedures. Initially, tissue segmentation is executed automatically on each slide at a reduced magnification. This involves generating a binary mask for the tissue regions by applying a binary threshold to the saturation channel of the downsampled image, following its conversion from RGB to HSV color space. Morphological closing and median blurring are employed for smoothing the contours of the detected tissue and minimizing artifacts. Subsequently, the approximate contours of both the tissue and the tissue cavities are assessed and filtered based on their area, culminating in the creation of the final segmentation mask.

We complete set of pre-processing hyperparameters for optimization in histopathological tasks is thus $H_n = [x_1, x_2, x_3, x_4, x_5, x_6]$, where each x_i has its own hyper-parameter space. As illustrated in Fig 4 and the observations discussed in Section 3, the set of pre-processing hyperparameters affect the performance together, varying across the different datasets. A large area of tissue is detected as background or holes and then dropped during the pre-processing. As illustrated in Fig 4, dropping too many patches decreases performance in Fig. 4(a) and (c) but increases performance in Fig. 4(b) where the dataset is changed. It is hard and no work to measure how these patches and specific types of cells affect the out-of-domain inference performance in histopathological tasks. Thus, we optimize these histopathological tasks by machine learning

techniques instead of exploring the impact of the specific type of cells.

As illustrated in Fig 2, the hyper-parameter optimization for histopathological tasks is non-convex optimization which has many large local optima. Therefore, our goal is to search for an optimal hyper-parameter in a short time and with less cost; the optima we search for can just be larger as it can. We are not searching for the global optima. We just search for an optimal value much better than the default hyper-parameter in a very short time and cost. In practice, this involves repeatedly applying different features within the same foundational model using various hyperparameters H_n^* . Therefore, we propose a PSNR mechanism as a threshold to advance the speed of hyper-parameter search.

4.3. Optimization of Fast Hyper-Parameter Search

4.3.1. Good Pre-Processed WSIs show High Structural Similarity.

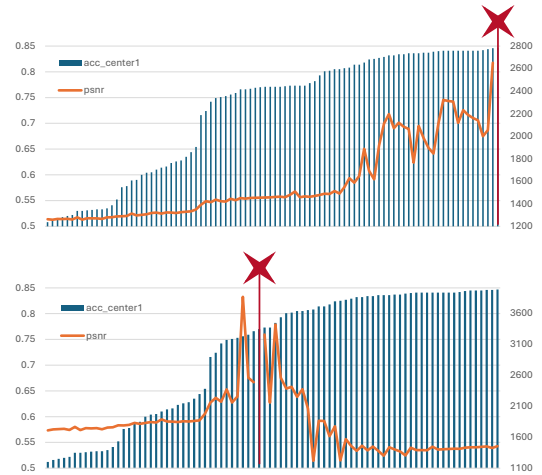


Figure 5. Relationship between PSNR and Accuracy. The red star stands for the reference object. All the hyper-parameters are compared with the reference object to calculate the PSNR.

For single-domain inference performance, our experiments demonstrate that pre-processing parameters, which lead to similar high accuracy, also generate the pre-processed images with similar structures (as illustrated in Figure 5). When the two objects are close in accuracy, their PSNR is always high. This phenomenon always exists, no matter how we change the reference object.

Therefore, we only evaluate the pre-processed Whole Slide Images (WSIs) that closely resemble the current optimally pre-processed WSI in each optimization iteration. To quantitatively assess differences between two sets of pre-processing results, we use Peak Signal-to-Noise Ratio (PSNR) to measure the similarity of images generated during patch creation. The general histopathological workflow

includes creating patches, extracting features, training models, and testing inference data. During patch generation, thumbnails are created for visualizing the preprocessing effects. Thumbnails are 64x downsampled from original gigapixel WSIs. Thus, we can determine the similarity between these two sets of pre-processed results by calculating PSNR for these thumbnails efficiently.

4.3.2. Peak Signal-to-Noise Ratio (PSNR)

Peak Signal-to-Noise Ratio (PSNR) is a common measurement in image processing and digital signal processing. A higher PSNR value indicates greater similarity between two images. We calculate the PSNR by comparing thumbnails generated during preprocessing. For example, the total PSNR of thumbnails produced using the second-best preprocessing parameters should be higher than that of any other set, as illustrated in Figure 5.

4.3.3. PSNR-based Basin Hopping for Hyper-Parameter Optimization

Algorithm 1 PSNR-based Basin Hopping Hyper-Parameter Optimization (BAHOP)

Input: Default parameter H_{train} with result set \mathcal{R} , Hyper-parameters space Φ , initial similarity threshold τ , function $Infer$ to evaluate performance, function S to calculate similarity

Output: Optimal parameters H^*

```

1: Initialize  $H^*$  with fixed default parameter  $H_{train}$ 
2: Generate pre-processed thumbnails  $I^*$  from  $H^*$  (for all validation WSIs)
3: Generate feature  $F^*$  from WSIs with  $H^*$ 
4:  $y^* \leftarrow Infer(F^*)$ 
5:  $\mathcal{R} \leftarrow (H^*, y^*)$ 
6: while optimization times do
7:   Select  $H_{new}$  by perturbing  $H^*$  slightly from  $\Phi$ 
8:   if  $H_{new}$  not in  $\mathcal{R}$  then
9:     Generate thumbnails  $I_{new}$  with  $H_{new}$ 
10:    if  $S(I_{new}, I^*) > \tau$  then
11:      Extract feature  $F_{new}$   $\triangleright$  Expensive step
12:       $y_{new} \leftarrow Infer(F_{new})$ 
13:       $\mathcal{R} \leftarrow \mathcal{R} \cup (H_{new}, y_{new})$ 
14:      if  $y_{new} > y^*$  then
15:         $H^*, I^*, y^* \leftarrow H_{new}, I_{new}, y_{new}$ 
16:      end if
17:    end if
18:  end if
19: end while
20: return  $H^*$ 

```

Basin-hopping is a global optimization technique characterized by iterative processes involving random perturbation of coordinates, followed by localized optimization and subsequent evaluation and acceptance or rejection of

new coordinates based on minimized function values. This method is particularly useful in high-dimensional landscapes. However, an inherent limitation of Basin-hopping lies in the necessity to execute random perturbations at a designated point, typically a local minimum. These perturbations must be suitably sized - adequately large to escape the current local minimum yet not excessively to devolve into total randomness. To address this challenge, we introduce a Peak Signal-to-Noise Ratio (PSNR) threshold within the Basin-hopping optimization process. Subsequently, our experimental endeavors focus on establishing a correlation between pre-processing methodologies applied to whole slide images and the PSNR metric.

The integration of PSNR-based filtering does not fundamentally change the Basin Hopping process itself but rather serves as a heuristic pre-processing step to enhance efficiency and fit histopathological tasks. The PSNR threshold is set dynamically and adapts across different datasets. The experiments of the effect of each pre-processing parameter are shown in the Appendix. From the experiments (as shown in the Appendix), the criteria for selecting the PSNR threshold and dynamically adapting to different datasets is that we perturb the pre-processing parameter – segmentation threshold (related to foreground and background detection). Each time, we change the value to plus or minus 1. We calculate the PSNR for this comparison as the initial PSNR. This process only requires the creation of a patch and quick PSNR calculation in thumbnails.

Also, we delete the mechanism of temperature and accepted probability from the original Basin hopping, ensuring our BAHOP is designed properly for histopathological tasks. For our proposed BAHOP method (as shown in Algorithm 1), we use H_{train} as the default parameter. Using the current optimal parameter H^* , we generate a new parameter H_{new} , create patches, and calculate their PSNR against the optimal thumbnails I^* . If the PSNR exceeds threshold τ , we proceed to more resource-intensive tasks such as feature extraction in histopathological analysis and subsequent inference using an existing model. Each new parameter set H_{new} is added to our historical dataset $R = \{(H_1, y_1), \dots, (H_i, y_i)\}$. If H_{new} demonstrates improved performance, H_* will be updated with H_{new} .

5. Experiments

5.1. Experiments Setup

Our experiment utilizes the pre-processing pipeline from CLAM [17]. The datasets include Camelyon 16, Camelyon 17 [16], TCGA-NSCLC, TCGA-BRCA, and TCGA-COAD [29]. For Camelyon16 and Camelyon17, we focus on normal-tumor classification; for all TCGA datasets, we address cancer subtype tasks. In our experiments, we fix the seeds and model hyperparameters such as learning rate

Model	TCGA-COAD					TCGA-BRCA				
	Center	Accuracy		AUC		Center	Accuracy		AUC	
		Default	Ours	Default	Ours		Default	Ours	Default	Ours
ABMIL [12]	CM	0.75	0.778	0.828	0.838	A7	0.902	0.961	0.964	0.994
	D5	0.709	0.774	0.64	0.647	AC	0.775	0.805	0.728	0.761
	DM	0.783	0.826	0.732	0.759	AR	0.781	0.816	0.834	0.856
	G4	0.963	0.963	0.98	1	C8	0.907	0.93	0.867	0.908
DSMIL [15]	CM	0.75	0.778	0.848	0.859	A7	0.921	0.941	0.923	0.962
	D5	0.806	0.871	0.5	0.493	AC	0.725	0.805	0.761	0.761
	DM	0.869	0.869	0.777	0.804	AR	0.765	0.781	0.733	0.738
	G4	0.963	0.963	0.96	0.98	C8	0.581	0.813	0.767	0.75
CLAM [17]	CM	0.75	0.889	0.56	0.636	A7	0.941	0.961	0.947	0.974
	D5	0.742	0.871	0.46	0.793	AC	0.75	0.81	0.772	0.761
	DM	0.739	0.739	0.571	0.571	AR	0.813	0.828	0.882	0.878
	G4	0.889	0.926	0.94	0.96	C8	0.907	0.93	0.867	0.875
BayesMIL [5]	CM	0.861	0.889	0.929	0.929	A7	0.882	0.882	0.934	0.955
	D5	0.709	0.806	0.667	0.593	AC	0.775	0.775	0.799	0.821
	DM	0.783	0.826	0.821	0.875	AR	0.813	0.828	0.796	0.791
	G4	0.926	1	0.96	1	C8	0.86	0.884	0.792	0.767
MHIM-DSMIL [23]	CM	0.75	0.801	0.77	0.798	A7	0.923	0.961	0.957	0.996
	D5	0.839	0.871	0.48	0.493	AC	0.75	0.775	0.611	0.745
	DM	0.826	0.87	0.714	0.786	AR	0.75	0.766	0.709	0.713
	G4	0.925	0.963	0.94	0.98	C8	0.907	0.93	0.742	0.733

Table 2. **Experiments about out-of-domain inference performance in TCGA-COAD and TCGA-BRCA for cancer subtype.** We compare the accuracy obtained by default hyper-parameters with the optimal hyper-parameter searched by our BAHOP algorithm.

Model	Out-of-Domain(Center 0)				Out-of-Domain(Center 1)				Out-of-Domain(Center 4)			
	Accuracy		AUC		Accuracy		AUC		Accuracy		AUC	
	Def	Ours	Def	Ours	Def	Ours	Def	Ours	Def	Ours	Def	Ours
ABMIL [12]	0.93	0.97	0.921	0.965	0.84	0.92	0.833	0.896	0.88	0.93	0.907	0.911
DSMIL [15]	0.77	0.96	0.88	0.937	0.64	0.89	0.721	0.93	0.92	0.96	0.952	0.947
CLAM [17]	0.92	0.95	0.919	0.963	0.512	0.846	0.708	0.833	0.874	0.92	0.904	0.941
Bayes-MIL [5]	0.83	0.94	0.956	0.884	0.35	0.80	0.819	0.881	0.85	0.92	0.931	0.899
MHIM-DSMIL [23]	0.87	0.96	0.911	0.956	0.77	0.87	0.85	0.921	0.91	0.94	0.949	0.955

Table 3. Out-of-domain inference performance in **Center 0, center1 and Center 4 of Camelyon17** for normal and tumor classification.

and loss weight across similar tasks within the same model framework. Additional experimental details are provided in the Appendix. We employ K-fold, Stratified K-Fold or K-fold Monte Carlo cross-validation methods (with k sets to 10) to train models and assess out-of-domain performance. All results presented in Table 2, Table 3 and Table 4 represent average accuracy calculated over 10-fold models.

5.2. Classification Accuracy Validation of BAHOP

For the Camelyon datasets, we use 270 WSIs from Camelyon 16 to train the model and test inference performance across various centers in Camelyon17 to simulate out-of-domain scenarios. It’s important to note that Camelyon16 data was collected from two centers (UMCU and RUMC), while Camelyon17 includes data from five centers (CWZ,

RST, UMCU, RUMC, and LPON). Consequently, only centers 0 (CWZ), center 1 (RST), and center 4 (LPON) of Camelyon17 represent out-of-domain situations.

We compare inference performance using features extracted by default parameters (not the worst) and those optimized through our BAHOP algorithm. As shown in Table 2 and Table 3, the optimal hyper-parameters identified by our BAHOP algorithm generally surpass the default settings across various models and datasets. In specific cases, such as CLAM and BayesMIL at Center 1 of Camelyon 17, performance improved dramatically from 0.512 to 0.847 simply by adjusting the hyper-parameters.

For TCGA datasets, we divide the entire dataset according to TCGA Tissue Source Site Codes [29]. We select several centers with sufficient WSIs to form the testing

sub-dataset, while the remaining data constitutes the training dataset. The out-of-domain inference performance also improves (as shown in Table 2), indicating that our issue is general and our BAHOP provides a universal solution. Additionally, we conduct experiments on a larger TCGA-NSCLC dataset that includes more extensive out-of-domain testing (as detailed in Table 4).

TCGA-NSCLC						
Center	ABMIL [12]		CLAM [17]		Bayes-MIL [5]	
	Def.	Ours	Def.	Ours	Def.	Ours
21	0.72	0.78	0.56	0.78	0.56	0.67
22	0.87	0.89	0.78	0.84	0.84	0.84
43	0.75	0.80	0.60	0.75	0.70	0.80
49	0.59	0.64	0.69	0.71	0.71	0.76
55	0.49	0.52	0.66	0.76	0.28	0.33
77	0.93	0.93	0.91	0.93	0.75	0.80
97	1.00	1.00	0.91	1.00	0.87	0.96

Table 4. Comparison of inference accuracy in TCGA-NSCLC with more centers. Only accuracy is reported since each separate center only has one category. Def. stands for default parameter.

5.3. Comparison of other hyper-parameter optimization

As illustrated in Table 5, we compare different hyper-parameter optimization (HPO) techniques in one center of Camelyon 17 over 100 iterations. Our BAHOP can find the optimal hyper-parameters much quicker compared to alternative HPO methodologies. While other HPO techniques demonstrated the capability to achieve commendable accuracy levels, they incurred substantial costs in terms of computational time and resource utilization.

Table 5. Comparison of other hyper-parameter optimization. SA stands for Simulated Annealing. Lat. stands for Latency (smaller is better) and Mem. stands for Memory.

Strategy	Acc	Lat.(min)	Mem.(GB)
Random search	0.845	9600	1250
Grid search	0.847	9600	1250
SA [27]	0.846	9600	1250
Bayes OPT [22]	0.834	9600	1250
BAHOP (Ours)	0.846	1770	170

5.4. Efficiency Validation

Figure 6 shows the running time for optimizing preprocessing parameters 100 times. Our PSNR-based Basin Hopping (BAHOP) algorithm for Parameter Tuning uses PSNR to compare each pre-processed WSIs with the best one so far, selecting only those with high similarity for further feature extraction. WSIs with low PSNR are skipped, streamlining

the process and ensuring that only promising candidates are evaluated further. This approach prevents our BAHOP from getting stuck in local optima and saves time by reducing unnecessary feature extractions.

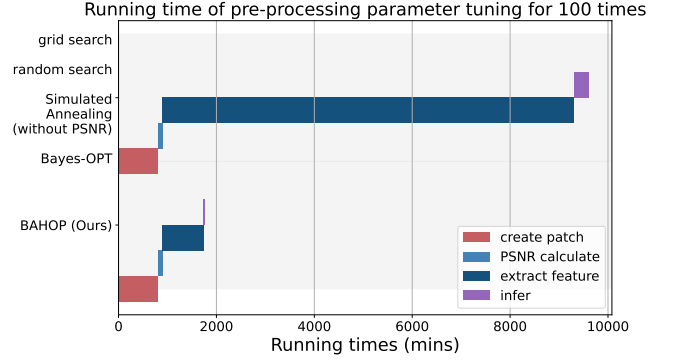


Figure 6. The running time of pre-processing parameters tuning for 100 times. Our algorithm can save time by skipping a large number of feature extraction.

5.5. Ablation Study

Strategy 1: PSNR The workflow of inference in histopathological tasks includes creating patches, extracting features, and inferred in a pre-trained model. Without the PSNR-based strategy, the algorithm will run the most expensive step – feature extraction, for each iteration. Our PSNR mechanism can skip feature extraction in many iterations (as shown in Table 6).

Strategy 2: Basin Hopping Basin Hopping prevents optimization from getting stuck in local optima. As illustrated in Table 5, search algorithms lacking Basin Hopping repeatedly test hyper-parameters that yield a higher PSNR than the current optimal solution. Since other optimization techniques have optimized for 100 times, the optimal accuracy is all high but the costs are so huge both in time and disk space.

Table 6. Ablation Study of the PSNR and Basin Hopping. Results are based on optimizing 100 times in the center1 of Camelyon 17. Lat. stands for Latency (smaller is better) and Mem. stands for Memory.

PSNR	BH	Acc	Lat. (min)	Mem. (GB)
✗	✓	0.846	9600	1250
✓	✗	0.845	2553	278
✓	✓	0.846	1770	170

6. Conclusion

Different pre-processing parameters significantly impact feature extraction and model performance in histopathological tasks. In this paper, we propose the Similarity-based Basin Hopping (BAHOP) algorithm for fast parameter tuning, which enhances inference performance on out-of-domain data. BAHOP achieves a 5% to 30% accuracy improvement on the Camelyon and multiple TCGA datasets, offering faster hyper-parameter search by reducing feature extraction steps based on WSI characteristics.

References

- [1] Amina Asif, Kashif Rajpoot, Simon Graham, David Snead, Fayyaz Minhas, and Nasir Rajpoot. Unleashing the potential of ai for pathology: challenges and recommendations. *The Journal of Pathology*, 260(5):564–577, 2023. [2](#)
- [2] Gabriele Campanella, Matthew G Hanna, Luke Geneslaw, Allen Miralflor, Vitor Werneck Krauss Silva, Klaus J Busam, Edi Brogi, Victor E Reuter, David S Klimstra, and Thomas J Fuchs. Clinical-grade computational pathology using weakly supervised deep learning on whole slide images. *Nature medicine*, 25(8):1301–1309, 2019. [1](#)
- [3] Caroline Choi, Yoonho Lee, Annie Chen, Allan Zhou, Aditi Raghunathan, and Chelsea Finn. Autoft: Robust fine-tuning by optimizing hyperparameters on ood data. *arXiv preprint arXiv:2401.10220*, 2024. [2](#), [3](#)
- [4] Didem Cifci, Gregory P Veldhuizen, Sebastian Foersch, and Jakob Nikolas Kather. Ai in computational pathology of cancer: improving diagnostic workflows and clinical outcomes? *Annual Review of Cancer Biology*, 7(1):57–71, 2023. [3](#)
- [5] Yufei Cui, Ziquan Liu, Xiangyu Liu, Xue Liu, Cong Wang, Tei-Wei Kuo, Chun Jason Xue, and Antoni B Chan. Bayesmil: A new probabilistic perspective on attention-based multiple instance learning for whole slide images. In *11th International Conference on Learning Representations (ICLR 2023)*, 2023. [2](#), [7](#), [8](#)
- [6] Taher Dehkharghanian, Azam Asilian Bidgoli, Abtin Riasatian, Pooria Mazaheri, Clinton JV Campbell, Liron Pantanowitz, HR Tizhoosh, and Shahryar Rahnamayan. Biased data, biased ai: deep networks predict the acquisition site of tcga images. *Diagnostic pathology*, 18(1):67, 2023. [1](#), [2](#), [3](#)
- [7] Amelie Echle, Niklas Timon Rindtorff, Titus Josef Brinker, Tom Luedde, Alexander Thomas Pearson, and Jakob Nikolas Kather. Deep learning in cancer pathology: a new generation of clinical biomarkers. *British journal of cancer*, 124(4):686–696, 2021. [3](#)
- [8] Stefan Falkner, Aaron Klein, and Frank Hutter. Bohb: Robust and efficient hyperparameter optimization at scale. In *International conference on machine learning*, pages 1437–1446. PMLR, 2018. [3](#)
- [9] Metin N Gurcan, Laura E Boucheron, Ali Can, Anant Madabhushi, Nasir M Rajpoot, and Bulent Yener. Histopathological image analysis: A review. *IEEE reviews in biomedical engineering*, 2:147–171, 2009. [2](#)
- [10] Mahdi S Hosseini, Babak Ehteshami Bejnordi, Vincent Quoc-Huy Trinh, Lyndon Chan, Danial Hasan, Xingwen Li, Stephen Yang, Taehyo Kim, Haochen Zhang, Theodore Wu, et al. Computational pathology: a survey review and the way forward. *Journal of Pathology Informatics*, page 100357, 2024. [3](#)
- [11] Frederick M Howard, James Dolezal, Sara Kochanny, Jeffrey Schulte, Heather Chen, Lara Heij, Dezheng Huo, Rita Nanda, Olufunmilayo I Olopade, Jakob N Kather, et al. The impact of site-specific digital histology signatures on deep learning model accuracy and bias. *Nature communications*, 12(1):4423, 2021. [1](#), [2](#), [3](#)
- [12] Maximilian Ilse, Jakub Tomczak, and Max Welling. Attention-based deep multiple instance learning. In *International conference on machine learning*, pages 2127–2136. PMLR, 2018. [7](#), [8](#)
- [13] Syed Ashar Javed, Dinkar Juyal, Harshith Padigela, Amaro Taylor-Weiner, Limin Yu, and Aaditya Prakash. Additive mil: Intrinsically interpretable multiple instance learning for pathology. *Advances in Neural Information Processing Systems*, 35:20689–20702, 2022. [4](#)
- [14] Yongju Lee, Jeong Hwan Park, Sohee Oh, Kyoungseob Shin, Jiye Sun, Minsun Jung, Cheol Lee, Hyojin Kim, Jin-Haeng Chung, Kyung Chul Moon, et al. Derivation of prognostic contextual histopathological features from whole-slide images of tumours via graph deep learning. *Nature Biomedical Engineering*, pages 1–15, 2022. [2](#)
- [15] Bin Li, Yin Li, and Kevin W Eliceiri. Dual-stream multiple instance learning network for whole slide image classification with self-supervised contrastive learning. In *Proceedings of the IEEE/CVF conference on computer vision and pattern recognition*, pages 14318–14328, 2021. [1](#), [2](#), [7](#)
- [16] Geert Litjens, Peter Bandi, Babak Ehteshami Bejnordi, Oscar Geessink, Maschenka Balkenhol, Peter Bult, Altuna Halilovic, Meyke Hermesen, Rob van de Loo, Rob Vogels, et al. 1399 h&e-stained sentinel lymph node sections of breast cancer patients: the camelyon dataset. *GigaScience*, 7(6):giy065, 2018. [1](#), [2](#), [6](#)
- [17] Ming Y Lu, Drew FK Williamson, Tiffany Y Chen, Richard J Chen, Matteo Barbieri, and Faisal Mahmood. Data-efficient and weakly supervised computational pathology on whole-slide images. *Nature biomedical engineering*, 5(6):555–570, 2021. [1](#), [2](#), [3](#), [6](#), [7](#), [8](#)
- [18] Milda Pocevičiūtė, Gabriel Eilertsen, Stina Garvin, and Claes Lundström. Detecting domain shift in multiple instance learning for digital pathology using fr chet domain distance. In *International Conference on Medical Image Computing and Computer-Assisted Intervention*, pages 157–167. Springer, 2023. [2](#), [3](#)
- [19] Maithra Raghu, Chiyuan Zhang, Jon Kleinberg, and Samy Bengio. Transfusion: Understanding transfer learning for medical imaging. *Advances in neural information processing systems*, 32, 2019. [3](#)
- [20] Massimo Salvi, U Rajendra Acharya, Filippo Molinari, and Kristen M Meiburger. The impact of pre-and post-image processing techniques on deep learning frameworks: A comprehensive review for digital pathology image analysis. *Computers in Biology and Medicine*, 128:104129, 2021. [2](#)
- [21] Zhuchen Shao, Hao Bian, Yang Chen, Yifeng Wang, Jian Zhang, Xiangyang Ji, et al. Transmil: Transformer based

- correlated multiple instance learning for whole slide image classification. *Advances in neural information processing systems*, 34:2136–2147, 2021. [1](#)
- [22] Jasper Snoek, Hugo Larochelle, and Ryan P Adams. Practical bayesian optimization of machine learning algorithms. *Advances in neural information processing systems*, 25, 2012. [8](#)
- [23] Wenhao Tang, Sheng Huang, Xiaoxian Zhang, Fengtao Zhou, Yi Zhang, and Bo Liu. Multiple instance learning framework with masked hard instance mining for whole slide image classification. In *Proceedings of the IEEE/CVF International Conference on Computer Vision*, pages 4078–4087, 2023. [1](#), [7](#)
- [24] David Tellez, Geert Litjens, Péter Bándi, Wouter Bulten, John-Melle Bokhorst, Francesco Ciompi, and Jeroen Van Der Laak. Quantifying the effects of data augmentation and stain color normalization in convolutional neural networks for computational pathology. *Medical image analysis*, 58: 101544, 2019. [2](#)
- [25] Antonio Torralba and Alexei A Efros. Unbiased look at dataset bias. In *CVPR 2011*, pages 1521–1528. IEEE, 2011. [3](#)
- [26] Jeroen Van der Laak, Geert Litjens, and Francesco Ciompi. Deep learning in histopathology: the path to the clinic. *Nature medicine*, 27(5):775–784, 2021. [1](#)
- [27] Peter JM Van Laarhoven, Emile HL Aarts, Peter JM van Laarhoven, and Emile HL Aarts. *Simulated annealing*. Springer, 1987. [8](#)
- [28] Jun Wang, Yu Mao, Nan Guan, and Chun Jason Xue. Advances in multiple instance learning for whole slide image analysis: Techniques, challenges, and future directions. *arXiv preprint arXiv:2408.09476*, 2024. [2](#)
- [29] John N Weinstein, Eric A Collisson, Gordon B Mills, Kenna R Shaw, Brad A Ozenberger, Kyle Ellrott, Ilya Shmulevich, Chris Sander, and Joshua M Stuart. The cancer genome atlas pan-cancer analysis project. *Nature genetics*, 45(10):1113–1120, 2013. [2](#), [6](#), [7](#)
- [30] Yukako Yagi. Color standardization and optimization in whole slide imaging. In *Diagnostic pathology*, pages 1–12. Springer, 2011. [2](#)
- [31] Hongrun Zhang, Yanda Meng, Yitian Zhao, Yihong Qiao, Xiaoyun Yang, Sarah E Coupland, and Yalin Zheng. Dtf-dmil: Double-tier feature distillation multiple instance learning for histopathology whole slide image classification. In *Proceedings of the IEEE/CVF Conference on Computer Vision and Pattern Recognition*, pages 18802–18812, 2022. [1](#)